nature physics

ARTICLES

PUBLISHED ONLINE: 4 OCTOBER 2009 | DOI: 10.1038/NPHYS1403

Emergent crystallinity and frustration with Bose–Einstein condensates in multimode cavities

Sarang Gopalakrishnan[1,2]*, Benjamin L. Lev[1] and Paul M. Goldbart[1,2,3]

We propose that condensed-matter phenomena involving the spontaneous emergence and dynamics of crystal lattices can be realized using Bose–Einstein condensates coupled to multimode optical cavities. It is known that, in the case of a transversely pumped single-mode cavity, the atoms crystallize at either the even or the odd antinodes of the cavity mode at sufficient pump laser intensity, thus spontaneously breaking a discrete translational symmetry. Here we demonstrate that, in multimode cavities, crystallization involves the spontaneous breaking of a continuous translational symmetry, through a variant of Brazovskii's transition, thus paving the way for realizations of compliant lattices and associated phenomena, such as dislocations, frustration, glassiness and even supersolidity, in ultracold atomic settings, where quantum effects have a dominant role. We apply a functional-integral formalism to explore the role of fluctuations in this correlated many-body system, to calculate their effect on the threshold for ordering, and to determine their imprint on the correlations of the light emitted from the cavity.

Since the development of modern laser cooling and trapping techniques, a range of phenomena associated with condensed-matter physics have been realized in ultracold atomic systems. The value of these realizations stems from their superb tunability and purity. Systems realized, so far, frequently involve externally imposed periodic potentials to simulate, for example, electrons in static crystal lattices or low-dimensional quantum fluids. Many areas of condensed matter—for example, soft matter, glassiness and supersolidity[1]—have, however, remained inaccessible to ultracold atomic physics, because the lattices realized have been imposed externally using lasers, rather than arising spontaneously from many-body effects. Therefore, it has not yet proved possible to realize phenomena that depend on the presence of an emergent, compliant lattice, capable of exhibiting, for example, dynamics, defects and melting. Tunable ultracold atomic versions of such phenomena are welcome because several fundamental issues remain unresolved, such as the dynamics of glassy media.

A major advance towards self-generated, dynamical optical lattices was the discovery of cavity-induced self-organization[2–5]. Consider N two-level atoms in a single-mode optical cavity, interacting with the cavity mode and a pump laser oriented transverse to the cavity axis. The atoms coherently scatter light between the pump and cavity modes. Atoms arranged at every other antinode of the cavity field (that is, one cavity-mode wavelength λ apart) emit in phase and populate the cavity with photons, leading to the collective, superradiant enhancement of the atom–cavity coupling by a factor proportional to the number of organized atoms. If the pump laser has sufficient intensity and is red-detuned from the atomic transition (so that the atoms are attracted to field-intensity maxima), an instability arises: λ-period fluctuations of the atomic density trigger superradiance, which enhances the atom–cavity coupling and further traps the atoms in λ-spaced wells at either the even or odd antinodes. This leads to greater superradiance, stronger atomic trapping and so on. The system reaches a spatially modulated steady state when the energy gain from superradiance is balanced by the cost, in kinetic energy or repulsive interactions, of confining the atoms to the even or the odd sites of the emergent lattice. Signatures of this non-equilibrium phase transition have been observed experimentally[6], and it has an important role in schemes for cooling exotic atomic or molecular species[7,8].

Single-mode cavities, unlike artificial optical lattices, feature an emergent lattice depth and a discrete symmetry breaking between even and odd antinode ordering. However, the locations of the antinodes are not themselves emergent, instead being fixed by the cavity geometry. In contrast, even in the simplest multimode cavity (that is, the ring cavity, which supports two counterpropagating modes[9]), the atoms collectively fix the locations of the antinodes, thus spontaneously breaking a continuous translational symmetry. As with real crystals, this results in an emergent rigidity with respect to lattice deformations. In cavities possessing many degenerate modes, one can anticipate realizing further phenomena associated with crystallizing systems, including topological defects such as dislocations and domain walls.

The purpose of this article is to develop and apply a field-theoretical framework for exploring the quantum statistical mechanics of correlated many-atom, many-photon systems in multimode cavities. This framework enables us to treat phenomena such as quantum phase transitions exhibited by the atom–cavity system and, in particular, to analyse the consequences of collective fluctuations, which have a pivotal role in the formation of ordered states. We apply our framework to the case of a pancake-shaped Bose–Einstein condensate (BEC) confined in a concentric cavity (see Fig. 1), and find a transition to a spatially modulated state that realizes Brazovskii's transition[10] and persists to zero temperature, thus becoming a quantum phase transition of an unusual universality class. Furthermore, we discuss the imprint of the associated quantum fluctuations in the correlations of the light emitted from the cavity. Finally, we generalize our model to incorporate layered, three-dimensional (3D) distributions of atoms, and find that (in certain parameter regimes) such systems cannot order globally because of frustration, and are expected to develop inhomogeneous, static domains. Indications of such phenomena were observed in simulations

[1]Department of Physics; [2]Institute for Condensed Matter Theory; [3]Frederick Seitz Materials Research Laboratory, University of Illinois at Urbana-Champaign, Urbana, Illinois 61801, USA. *e-mail: sgopala2@illinois.edu.

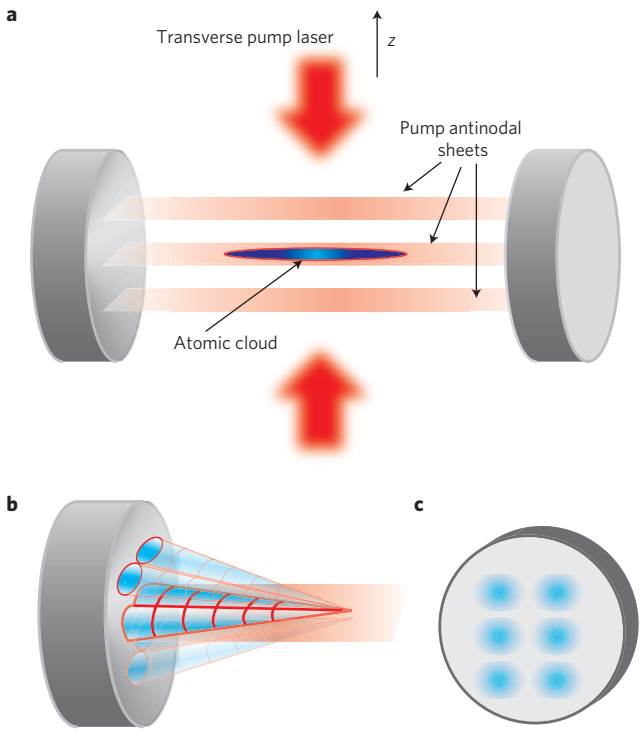

Figure 1 | The layered atom–cavity system. The cavity is transversely pumped by two counterpropagating lasers, which create a deep optical lattice and confine atoms at the antinodes of this lattice. **a**, The pump laser antinodes (red sheets) and the atomic BEC confined to a single equatorial sheet. **b**, The mode function labelled by $(l,m,n)=(2,1,5)$, or alternatively by TEM_{21}. The three numbers enumerate the nodes (one fewer than the number of lobes) in the pump (z), angular and radial directions, respectively. The radial mode number n is fixed by the requirement that $l+m+n$ be constant for a family of degenerate modes, and can therefore be omitted. **c**, The cross-section of mode TEM_{21} at one of the end mirrors.

(H. Ritsch, personal communication); in this work, we identify the origin of these domains.

Spatial ordering in multimode cavities is a form of supersolidity, because the ordered states are characterized by off-diagonal long-range order (arising from the BEC of the atoms) as well as emergent crystalline (that is, diagonal) order. A key difference between our system and those studied in refs 11 and 12 is that the solidity is associated with a spontaneously broken continuous symmetry, and can therefore be used to carry out ultracold atomic versions of experiments studying the transport properties of supersolids[1].

Elements of the model

The system discussed here comprises N two-level bosonic atoms confined in a multimode optical cavity and pumped transversely by lasers. In addition to having cavity-mediated interactions, the atoms repel each other by means of a contact interaction of strength U; we focus on the case of Bose-condensed atoms, but the self-organization phenomenon is not restricted to condensates. For simplicity, we address one particular kind of multimode cavity, namely the concentric cavity, which consists of two incomplete spherical mirrors with coincident centres of curvature. Perfectly concentric cavities lie at the stability boundary, but it is possible to make nearly concentric cavities having stable modes that are frequency-degenerate to within the cavity's linewidth. The analysis below focuses on concentric cavities because of their simple, spherical symmetry structure, but it applies qualitatively to any cavity having a large family of degenerate modes, for example, the confocal cavity.

We start with the Hamiltonian H for a 3D system of N identical two-level atoms, each of mass M and internal electronic energy-level spacing $\hbar\omega_A$, interacting with the degenerate cavity modes and a transverse pump field that varies spatially along the z direction[13]:

$$H = \sum_{i=1}^{N}\left[\frac{|\mathbf{p}_i|^2}{2M}+\hbar\omega_A\sigma_i^z\right]+U\sum_{1\le i<j\le N}\delta(\mathbf{x}_i-\mathbf{x}_j)$$
$$+\sum_{\alpha}\hbar\omega_C\, a_\alpha^\dagger a_\alpha + i\hbar\sum_{i=1}^{N}\sum_{\alpha}\left[g_\alpha(\mathbf{x}_i)\, a_\alpha^\dagger\, \sigma_i^- - \text{h.c.}\right]$$
$$+i\hbar\Omega\sum_{i=1}^{N}\cos(k_L z_i)(\sigma_i^- - \sigma_i^+)+H_{dis} \qquad (1)$$

The σ matrices are Pauli matrices acting on the internal state of the atoms; $\mathbf{x}_i$ and $\mathbf{p}_i$ are atomic positions and momenta; $\{a_\alpha\}$ are cavity-photon-annihilation operators for each mode α; $g_\alpha(\mathbf{x})\equiv g\,\Xi_\alpha(x)$, where g is the atom–cavity coupling strength and Ξ_α is the normalized mode function of mode $\alpha\equiv(l,m,n)$ (see Fig. 1b); Ω is the Rabi frequency (proportional to pump laser field); k_L is the pump laser wave vector; and H_{dis} consists of dissipative terms arising from the loss of intracavity photons through the cavity mirrors and from the spontaneous decay of the atomic excited state. The net rate of cavity loss is denoted κ (that is, the cavity's linewidth), and that of spontaneous decay γ; we return shortly to a more microscopic analysis of these dissipative terms.

We work in the rotating-wave approximation, and assume throughout that the pump laser frequency ω_L is red-detuned from the cavity mode by 10–100 MHz, and that both of these frequencies are substantially red-detuned from the atomic transition by 1–10 GHz, so that $\omega_L \gg (\omega_A-\omega_L) \gg (\omega_C-\omega_L) > 0$. We express the frequencies in terms of detunings $\Delta_A\equiv\omega_A-\omega_C\approx\omega_A-\omega_L$ and $\Delta_C\equiv\omega_C-\omega_L$.

To emphasize the spontaneity of the symmetry breaking, we initially assume that the atoms are confined to the 'equatorial' plane $z=0$ by the pump-laser-dipole potential (or by another laser). This situation, realizable through selective loading techniques[14], has the advantage that, below threshold, the condensate has no external forces acting on it in the $z=0$ plane, so that the choice of the mode into which the atoms self-organize is a strictly emergent process. Although a single-pancake cloud would certainly meet this requirement, so could a narrow, multi-pancake cloud, as long as the atomic distribution along z does not extend as far as the off-equator maxima of higher-order ($l\neq 0$) cavity modes along z (see Fig. 1). In the 'Frustration in layered systems' section, we relax this assumption and discuss the effects of 3D pump–cavity interference.

Effective atomic action

To account for the quantum statistics of the (bosonic) atoms, we work with second-quantized atomic fields, $\Psi_g(\mathbf{x})$ and $\Psi_e(\mathbf{x})$, for the ground and excited states of the atom, and at fixed chemical potential μ. Thus, the Hamiltonian (including the chemical potential term) becomes

$$\mathcal{H}=\int d^dx\begin{bmatrix}\Psi_g^\dagger & \Psi_e^\dagger\end{bmatrix}\begin{bmatrix}H_0 & H_{int}\\ H_{int}^\dagger & H_0+\hbar\omega_A\end{bmatrix}\begin{bmatrix}\Psi_g\\ \Psi_e\end{bmatrix} \qquad (2)$$

where all terms depend on $\mathbf{x}$, $H_0\equiv-\hbar^2\nabla^2/2M+U\,\Psi_g^\dagger(\mathbf{x})\,\Psi_g(\mathbf{x})-\mu$ and $H_{int}\equiv i\left(\Omega^*+\sum_\alpha g_\alpha(\mathbf{x})a_\alpha^\dagger\right)$. As the density of excited-state atoms is small, we have neglected their self-interactions.

We now reformulate our description of the system plus environment in terms of functional integrals, a procedure that is subtle because of the dissipative and driven nature of the system.

The standard formalism of quantum many-body theory[15] assumes that if interactions are turned on adiabatically in the distant past and turned off adiabatically in the distant future, the ground state of the non-interacting system evolves back to itself, up to a phase factor (that is, adiabatic switching). This assumption does not generically hold away from equilibrium: a completely general description of the coupled atom–cavity dynamics requires the Schwinger–Keldysh formalism[16,17], a straightforward extension of our approach that avoids this assumption. However, in the case at hand, the assumption of adiabatic switching holds to a good approximation near the threshold for self-organization, because the energy flux through the system is negligible on the timescales associated with the internal dynamics of the system. One can establish the validity of the aforementioned approximation within the Keldysh formalism; however, a more transparent argument that uses perturbation theory is given in the Supplementary Information.

We now transform to a frame rotating at the laser frequency ω_L, and write the coherent-state 'partition function'—neglecting spontaneous decay owing to large Δ_A—as a path integral over all of the atomic and photonic fields, with an action S that consists of atomic, electromagnetic (that is, cavity), interaction and dissipative parts:

$$S = S_{at} + S_{em} + S_{int} + S_{dis} \tag{3}$$

where

$$\begin{aligned}
S_{at} &\equiv \int d^d x\, d\tau \left[\Psi_g^*(\mathbf{x},\tau)\left(\partial_\tau - \frac{\hbar\nabla^2}{2M} - \frac{\mu}{\hbar}\right)\Psi_g(\mathbf{x},\tau) \right.\\
&\quad + \Psi_e^*(\mathbf{x},\tau)\left(\partial_\tau - \frac{\hbar\nabla^2}{2M} + \omega_A - \frac{\mu}{\hbar}\right)\Psi_e(\mathbf{x},\tau)\\
&\quad \left. + \frac{U}{\hbar}\,|\Psi_g(\mathbf{x},\tau)|^2\left(|\Psi_g(\mathbf{x},\tau)|^2 + |\Psi_e(\mathbf{x},\tau)|^2\right)\right]\\
S_{em} &\equiv \int d\tau \sum_\alpha a_\alpha^*(\tau)(\partial_\alpha + \omega_C)a_\alpha(\tau)\\
S_{int} &\equiv \int d\tau\, d\mathbf{x}\left[\sum_\alpha i g_\alpha(\mathbf{x})\,\Psi_e^*(\mathbf{x},\tau)\,\Psi_g(\mathbf{x},\tau)a_\alpha(\tau) + \text{h.c.}\right.\\
&\quad \left. + i\Omega\Psi_e^*(\mathbf{x},\tau)\,\Psi_g(\mathbf{x},\tau) + \text{h.c.}\right]\\
S_{dis} &\equiv \int d\tau \sum_\varepsilon A_\varepsilon^*(\partial_\tau + \omega_\varepsilon)A_\varepsilon + \sum_{\alpha,\varepsilon}\tilde{\kappa}_{\alpha,\varepsilon}a_\alpha^\dagger A_\varepsilon + \text{h.c.}
\end{aligned}$$

where A_ε denote free-space (that is, extracavity) environmental modes, and τ is imaginary time. We proceed as follows to develop an effective atom-only action (for details, see Supplementary Information): first, we carry out the Gaussian path integrals over Ψ_e and A_ε; next, we carry out the (also Gaussian) path integral over a_α, thus arriving at an action entirely in terms of the atomic motional states. Below threshold, this action has the form

$$\begin{aligned}
S_{eff} &= \sum_\nu \int d^d x\; \Psi^*(\omega_\nu,\mathbf{x})\left[i\omega_\nu - \frac{\hbar\nabla^2}{2M} - \frac{\mu}{\hbar}\right]\Psi(\omega_\nu,\mathbf{x})\\
&\quad - \zeta\sum_\alpha \int d\tau\, d^d x\, d^d x'\; \Xi_\alpha(\mathbf{x})\,|\Psi(\tau,\mathbf{x})|^2\,\Xi_\alpha^*(\mathbf{x}')\,|\Psi(\tau,\mathbf{x}')|^2\\
&\quad + \frac{U}{\hbar}\int d\tau\, d^d x\,|\Psi(\tau,\mathbf{x})|^4 + \cdots
\end{aligned} \tag{4}$$

where $\{\omega_\nu\}$ are Matsubara frequencies[18], which are Fourier conjugates of imaginary time, Ξ_α is the normalized mode function of mode α and the coupling constant $\zeta \equiv g^2\Omega^2\Delta_C/(\Delta_A^2(\Delta_C^2+\kappa^2))$. In taking S_{eff} to be the leading term, we have assumed that $\Omega_{th}^2 \geq g^2 N$; this assumption is generally satisfied (see the 'Experimental considerations' section).

Order-parameter formulation

We analyse the atom-only action by reformulating it in terms of an order parameter for self-organization into mode α; the natural choice for such an order parameter is the expectation value of the component of the atomic density modulation in mode α:

$$\langle\rho_\alpha\rangle \equiv \int d\mathbf{x}\,\langle|\Psi^*(\mathbf{x},\tau)|^2\rangle\,\Xi_\alpha(\mathbf{x}) \tag{5}$$

This resembles the order parameter for crystallization, except that for crystallization one typically has $\Xi_\alpha \equiv e^{i\mathbf{k}\cdot\mathbf{x}}$ (ref. 19). The mode structure of the concentric cavity, in contrast, is indexed by the integers (l,m,n) (see Fig. 1b). The family of cavity modes nearest the laser in frequency satisfy $2\pi(l+m+n) = K_0 R$, which is analogous to the dispersion relation $|\mathbf{k}|^2 = (\omega_C/c)^2$; these are the modes into which the atoms tend to crystallize. Of the modes with $2\pi(l+m+n) = K_0 R$, those with $l = 0$ have the largest amplitude near the equator, and are therefore the first to become unstable as the pump laser power is increased. Assuming that the atoms are spread out over a large number of optical wavelengths, we can use the asymptotic result

$$\int d\mathbf{x}\prod_i \Xi_{m_i n_i}(\mathbf{x}) \approx \delta_{\sum m_i,0}\,\delta_{\sum n_i,0} \tag{6}$$

which is the analogue of momentum conservation, to derive a Landau–Wilson action in terms of the order parameter. There are various cases, all qualitatively similar; we focus on the two simplest and most instructive ones: $T > 0$, in the absence of interactions, and $T = 0$, with repulsive interactions. In the former case (see Supplementary Information for details), we arrive at the action

$$\begin{aligned}
S_{LW} &= \sum_{mn}\left[\frac{r}{\chi} + \left(|m| + n - \frac{K_0 R}{2\pi}\right)^2\right]\rho_{mn}\rho_{-mn}\\
&\quad + \frac{4\zeta^2 N M^2}{\chi^2\hbar^2 K_0^4}\sum_{m_i n_i}\rho_{m_1 n_1}\rho_{m_2 n_2}\rho_{m_3 n_3}\rho_{m_4 n_4}\delta_{\sum m_i}\delta_{n_1+n_2,n_3+n_4}
\end{aligned} \tag{7}$$

where we have scaled ρ_{mn} to be dimensionless. The control parameter r is given by

$$r = 1 - \frac{N\zeta}{\hbar K_0^2/2M^2} \tag{8}$$

and χ is a parameter that describes the width about K_0 of the strip of atomic density modes for which the stability is reduced owing to intracavity-photon-mediated atom–atom interactions. Contributions to χ arise from the intrinsic linewidths of the cavity modes, their broadening owing to atom–cavity coupling and the coupling between the atoms and $l > 0$ cavity modes (which satisfy $2\pi(m+n) < K_0 R$). This action can be understood as follows: for $r > 0$, all density fluctuations cost energy, so the system does not self-organize. For $r < 0$, the system can lower its energy by forming a density wave of wave vector $2\pi(m+n) = K_0 R$, so the uniform state is unstable towards self-organization into one (or more) of the spatially modulated states having $2\pi(m+n) = K_0 R$; the extent of this modulation is determined by a competition between the quadratic and quartic terms in the action. The action has no cubic term

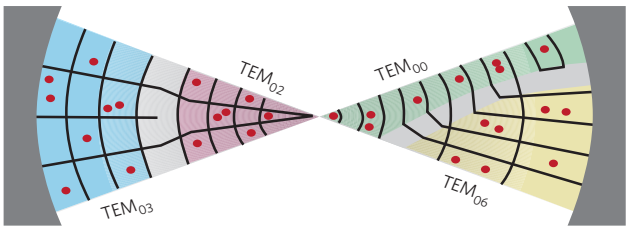

Figure 2 | Ordered state with defects. The ordered states form two-dimensional patterns. This diagram shows a regime near threshold, with domains locally populating distinct cavity modes at the equatorial plane. Domains can be punctuated by dislocations (shown in the left half of the figure), but might also show textural variation in space (right half of the figure). The black lines represent nodes of the cavity field, which separate 'even' and 'odd' antinodes. As the atoms are Bose-condensed, the atomic population per site is not fixed.

because, to satisfy 'momentum' conservation, such a term would have to involve at least one mode with $2\pi m \geq K_0 R/2$. However, modes with most of their structure in the angular (that is, large m) direction are suppressed because (1) such modes have higher diffractive losses[20] and (2) the atoms are confined to the intersection of pump and cavity modes (which lies near the centre of the cavity), and are therefore located mostly near modes with $m \ll n$.

Consequently, the effective action is not—as one might have expected—of the Landau form for crystallization[19], but is instead a variant of Brazovskii's action[10], which describes phase transitions from isotropic to striped structures in various condensed-matter settings, from diblock copolymers[21] to convective patterns[22]. Qualitatively, in these systems the uniform state becomes unstable to a density wave of wave vector k in any direction; the direction of ordering wanders across the sample, resulting in wavy lamellar patterns punctuated by defects. In our realization, the condensate becomes unstable towards self-organization into any mode with $2\pi(m+n) = K_0 R$; different regions organize into different modes, leading to a profusion of defect textures and dislocations, as shown in Fig. 2. In practice, the crystallizing states might not be exactly degenerate: for example, cavity modes of higher m are of lower finesse, whereas the repulsive interaction energy is greatest for atoms crystallizing into modes of lower m. Incorporating fictitious biasing fields into our model would account for such effects.

A distinctive feature of Brazovskii's transition is that, owing to the large manifold (in our case, a strip at $2\pi(m+n) \approx K_0 R$) of low-energy modes, fluctuations have an unusually strong role near the transition: they control not only the critical exponents, but even the order of the transition itself. The mean-field threshold Ω_{mf} for the pump intensity can be read off from the action S_{LW} by setting $r = 0$:

$$\frac{\hbar^2 K_0^2}{2M} = \frac{\hbar \Delta_{\mathrm{C}} g^2 \Omega_{\mathrm{mf}}^2}{\Delta_{\mathrm{A}}^2 (\Delta_{\mathrm{C}}^2 + \kappa^2)} N \tag{9}$$

This expression is the same as that derived in ref. 5 at zero temperature using the Gross–Pitaevskii equation; this is because at low temperatures ($T \leq T_{\mathrm{BEC}}$) it is primarily quantum effects that act to delocalize the BEC. Furthermore, mean-field theory predicts a continuous transition. However, the true threshold Ω_{th}, which follows from applying Brazovskii's scheme for including fluctuations in the action, is higher, and is given by the expression:

$$\Omega_{\mathrm{th}}^2 - \Omega_{\mathrm{mf}}^2 \sim \left[\frac{g^2 \Delta_{\mathrm{C}}}{\Delta_{\mathrm{A}}^2 (\Delta_{\mathrm{C}}^2 + \kappa^2)} \frac{\Omega_{\mathrm{th}}^8 M R^2}{\hbar N \chi} \right]^{\frac{1}{3}} \tag{10}$$

In addition, the transition is first-order: the order parameter jumps discontinuously from zero. As with other first-order transitions,

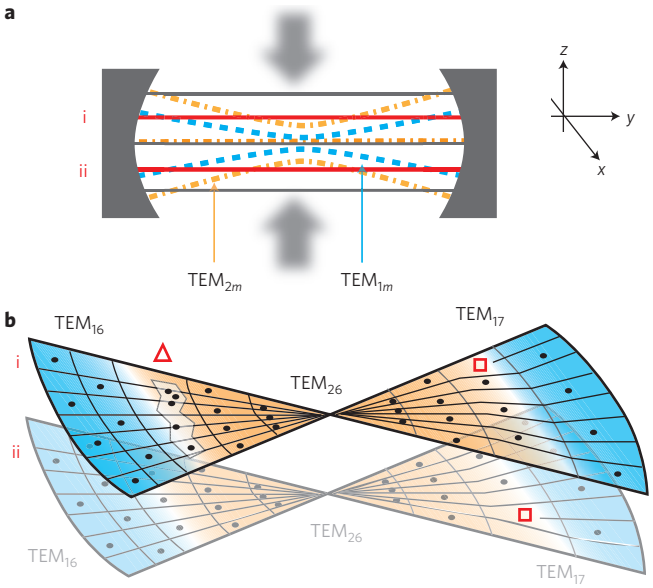

Figure 3 | Effects due to frustration. a, Atoms are loaded into sheets (i) and (ii), marked by thick red lines, which are an integer number of pump wavelengths apart. The blue (dashed) and orange (dash-dot) curves are, respectively, antinodal regions of the modes TEM_{1m}, which have low intensity near the centres of sheets (i) and (ii), and TEM_{2m}, which have low intensity away from the centres of sheets (i) and (ii). Near the centre of each sheet, atoms crystallize into TEM_{2m}; away from the centre, they crystallize into $\mathrm{TEM}_{1m'}$. **b**, Within a sheet, regions may be separated by a discommensuration, for example, in the left side of the figure, or a dislocation, for example, in the right side of the figure. Between sheets, the opposite parity of adjacent modes leads to frustration, which precludes ordering, as in the regions indicated by a triangle and a square. Dislocations (squares), being more localized, are less energetically costly than discommensurations (triangles).

Brazovskii's proceeds by the nucleation and growth of droplets of the stable phase. The morphology of these droplets is known to be rich: there are regimes dominated by anisotropic and diffuse droplets, as well as ones in which the droplets form 'focal conic' structures[23].

We now turn to the quantum phase transition at $T = 0$. As is generally the case at zero temperature, the effective action in this case involves an integral over the Matsubara frequency. An argument adapted from ref. 18 (see Supplementary Information) yields the effective low-frequency action:

$$S = \int \mathrm{d}\omega \sum_{mn} \frac{1}{\zeta} \left[r' + \omega^2 + \chi' (2\pi(m+n) - K_0 R)^2 \right] |B_{\omega mn}|^2 + \frac{U}{\hbar} \int \mathrm{d}\tilde{\tau}\, \mathrm{d}^2 x\, |B(\mathbf{x}, \tilde{\tau})|^4 + \cdots \tag{11}$$

where B describes the collective Bogoliubov excitations of the condensate, $r' \equiv (\hbar K_0^2/2M)^2 - (\zeta N \hbar K_0^2/2M)$ and χ' serves (as χ did in the classical case) as a broadening of the constraint $2\pi(m+n) \simeq K_0 R$. The extra dimension arising from the integral over ω changes the spectrum of fluctuations; instead of a ribbon of fluctuations, we must consider an anisotropic tube. In the extremely anisotropic limit, large χ' (achievable at very weak coupling to $l \neq 0$ modes), Brazovskii's argument applies once again; more generally, however, this phase transition is of an unusual and unfamiliar universality class. Power-counting arguments suggest that the variation of U or χ' might tune the system across a tri-critical point from a Brazovskii-like region to one in which

the transition is continuous. We shall address this issue using renormalization-group techniques in future work.

Experimental considerations

It is essential to any experimental realization of the above physics that the atoms stay Bose-condensed long enough for the slow dynamics of critical fluctuations to be observable. This is experimentally challenging because spontaneous emission, as well as the noise owing to the coupling between atoms and intracavity photon-number fluctuations, heats a BEC. The rate of heating by means of spontaneous decay is given by $R_\gamma \approx \gamma\,\Omega^2/4\Delta_A^2$; that due to fluctuations in cavity photon number, by[24]

$$R_c \approx R_\gamma \times \frac{\kappa^2}{\Delta_C^2} \times \frac{\sum_\alpha \langle n_\alpha \rangle}{N} \times \frac{g^2}{\kappa\gamma} \qquad (12)$$

Typical experimentally realizable parameters for a cavity quantum electrodynamics system showing these phase transitions might be $(g,\kappa,\gamma) = 2\pi(0.1, 0.1, 6)$ MHz (achievable using, for example, rubidium atoms in a 1 cm concentric cavity with mirrors of finesse 10^4); in addition, let us choose $\Delta_C = 2\pi \times 100$ MHz and $\Delta_A = 2\pi \times 10$ GHz, and the number of atoms $N = 10^5$. With these parameters, the laser strength at the mean-field threshold $\Omega_{th}^{mf} \approx 2\pi \times 100$ MHz, and the true laser threshold is higher by 1–5 MHz; therefore, $R_\gamma \approx 500$ Hz. Below threshold, when there are very few photons in the cavity, this is the dominant heating process. Above but near threshold, $n_\alpha = (g\,\Omega_{th}/\Delta_A\Delta_C)^2(\rho_{mn})^2 \sim 10^{-10}\rho_{mn}^2$, where $\rho_{mn} \ll N(= 10^5)$, so that $R_c \leq R_\gamma$ even in this regime. Heating is therefore dominated by spontaneous emission, and the criterion for the visibility of critical fluctuations—or other effects, such as supersolid correlations or glassy dynamics—is that they take place on timescales faster than 500 Hz. An estimate of the range of pump intensities for which critical fluctuations should be visible, that is, of the strength of critical effects, is given by the difference between the old and new thresholds (which can be obtained from equation (10)); for the above parameters, critical fluctuations are expected to have an important role for pump intensities $\Omega_{th}^{mf} \pm \Delta\Omega$, where $\Delta\Omega \approx 1 - 5$ MHz, which is much greater than the 500 Hz heating time and the typical laser intensity noise, and should therefore be observable.

Correlations of emitted light

The approach developed here can be used to compute atomic correlations by means of standard diagrammatic techniques; such correlations are experimentally obtainable as discussed in ref. 25. Furthermore, transmission through the cavity mirrors provides a real-time diagnostic channel for critical phenomena near threshold—for example, diverging correlation lengths and times—as well as supersolidity, in the spatial and temporal correlations of the light emitted from the cavity. Such correlations can be determined from the atomic correlations as explained in the Supplementary Information. The local variation in particle number that is characteristic of supersolidity should manifest itself, for example, in fluctuations in the spatial transmission pattern (as discussed in a different context in refs 26 and 27).

Frustration in layered systems

We have discussed how an equilibrium atomic cloud, confined by the pump laser to a plane near the equatorial plane of the cavity, spontaneously crystallizes globally into one of a family of degenerate checkerboard arrangements. Now let us consider an atomic cloud confined to a plane away from the equator of the cavity. In this case, spontaneous crystallization still occurs, but, as we shall now explain, the precise arrangement into which the atoms crystallize varies statically across the plane—for example, energetics demands that the centre and edge of the cloud crystallize in distinct arrangements. This is a consequence of frustration: satisfying local energetic preferences introduces 'fault zones' between locally ordered regions.

In our analysis of equatorial atomic distributions (see Fig. 2), we were able to restrict the family of modes considered to TEM_{lm} with $l = 0$. To generalize our analysis beyond the equatorial plane, we must consider all modes that meet the degeneracy condition $2\pi(l+m+n) \simeq K_0 R$. Consider the situation shown in Fig. 3a: near the centre of each sheet, crystallization into modes with $l = 2$ is favoured because such modes have high intensity; away from the centre, $l = 1$ modes are favoured. The change in l forces a change in m or n, owing to the degeneracy condition, so the mode functions in the sheet must change across an interfacial zone between the $l = 1$ and $l = 2$ regions. Therefore, either a dislocation (associated with a change in m) or a discommensuration, or change in lattice periodicity, associated with a change in n, is expected. Moreover, because odd- and even-l mode functions are of opposite parity about the $z = 0$ plane, the interfacial atoms at $-z$ suffer an energy cost whether they align or anti-align with those at $+z$; this cost can be mitigated through the introduction of dislocations, as shown in Fig. 3b. (For details see Supplementary Information.)

The full many-layer, many-mode system is expected to experience similar disordering effects to the idealization sketched above: that is, one expects systems slightly above threshold to develop locally crystalline phases separated by fault zones. It is plausible that these effects will lead, as they frequently do in condensed-matter systems, to glassiness.

Outlook

The formalism developed here enables one to explore the statics and slow collective dynamics of a BEC in a multimode cavity. This is sufficient for the exploration of critical fluctuations, which take place on extremely long timescales ($\geq 1/\kappa$ but $\leq 1/R_\gamma$, the heating time). To explore dynamics on shorter timescales (for example, defect motion), the formalism of this article can be extended using the Schwinger–Keldysh technique.

An experimentally relevant question is the extent to which the 'supersolidity' of BECs in multimode cavities enables one to test fundamental questions about supersolidity. A system well known in condensed-matter physics that may show supersolidity is solid ^{4}He, a phenomenon studied by 'missing moment of inertia' experiments[1]. Analogous experiments could be carried out using a self-organized BEC in a multimode cavity, and imparting angular momentum to the BEC, for example, by means of the pump laser.

Multimode cavity quantum electrodynamics provides a tunable setting in which self-organized states spontaneously break the continuous translational and/or orientational symmetries of space, rather than the discrete symmetry between the even and odd sites of either a single-mode cavity or an externally imposed lattice. This setting is expected to provide rich and fertile experimental terrain for probing quantum states of matter possessing emergent structural rigidity and superfluidity. Amongst other possibilities, compliant lattices offer the prospect of realizing fermionic superfluidity through phonon-mediated pairing of ultracold fermionic atoms.

Received 12 March 2009; accepted 25 August 2009; published online 4 October 2009

References

1. Kim, E. & Chan, M. H. W. Observation of superflow in solid helium. *Science* **305,** 1941–1944 (2004).
2. Domokos, P. & Ritsch, H. Collective cooling and self-organization of atoms in a cavity. *Phys. Rev. Lett.* **89,** 253003 (2002).
3. Asboth, J. K., Domokos, P., Ritsch, H. & Vukics, A. Self-organization of atoms in a cavity field: Threshold, bistability, and scaling laws. *Phys. Rev. A* **72,** 053417 (2005).

4. Lewenstein, M. *et al.* in *Proc. of ICAP Innsbruck* (eds Roos, C. F., Häffner, H. & Blatt, R.) 201–211 (AIP Conf. Proc. No. 869, AIP, 2006).
5. Nagy, D., Szirmai, G. & Domokos, P. Self-organization of a Bose–Einstein condensate in an optical cavity. *Eur. Phys. J. D* **48,** 127–137 (2008).
6. Black, A. T., Chan, H. W. & Vuletic, V. Observation of collective friction forces due to spatial self-organization of atoms: From Rayleigh to Bragg scattering. *Phys. Rev. Lett.* **91,** 203001 (2003).
7. Vuletic, V. & Chu, S. Laser cooling of atoms, ions, or molecules by coherent scattering. *Phys. Rev. Lett.* **84,** 3787–3790 (2000).
8. Lev, B. L. *et al.* Prospects for the cavity-assisted laser cooling of molecules. *Phys. Rev. A* **77,** 023402 (2008).
9. Nagy, D., Asboth, J. K., Domokos, P. & Ritsch, H. Self-organization of a laser-driven cold gas in a ring cavity. *Europhys. Lett.* **74,** 254–260 (2006).
10. Brazovskii, S. Phase transition of an isotropic system to an inhomogenous state. *Zh. Eksp. Teor. Fiz.* **68,** 175–185 (1975) (*Sov. Phys. JETP* **41**, 85–89 (1975)).
11. Góral, K., Santos, L. & Lewenstein, M. Quantum phases of dipolar bosons in optical lattices. *Phys. Rev. Lett.* **88,** 170406 (2002).
12. Yi, S., Li, T. & Sun, C. P. Novel quantum phases of dipolar Bose gases in optical lattices. *Phys. Rev. Lett.* **98,** 260405 (2007).
13. Walls, D. F. & Milburn, G. J. *Quantum Optics* (Springer, 2008).
14. Hadzibabic, Z., Krüger, P., Cheneau, M., Battelier, B. & Dalibard, J. Berezinskii–Kosterlitz–Thouless crossover in a trapped atomic gas. *Nature* **441,** 1118–1121 (2006).
15. Abrikosov, A., Gorkov, L. P. & Dzyaloshinski, I. E. *Methods of Quantum Field Theory in Statistical Physics* (Dover, 1975).
16. Keldysh, L. V. Diagram technique for nonequilibrium processes. *Sov. Phys. JETP* **20,** 1018–1025 (1965).
17. Kamenev, A. & Levchenko, A. Keldysh technique and nonlinear sigma-model: Basic principles and applications. *Adv. Phys.* **58,** 197–319 (2009).
18. Lifshitz, E. M. & Pitaevskii, L. P. *Statistical Physics, Part 2* (Course of Theoretical Physics, Vol. 9, Pergamon, 1980).
19. Alexander, S. & McTague, R. Should all crystals be bcc? Landau theory of solidification and crystal nucleation. *Phys. Rev. Lett.* **41,** 702–705 (1978).
20. Siegman, A. E. *Lasers* (University Science Books, 1986).
21. Leibler, L. Theory of microphase separation in block copolymers. *Macromolecules* **13,** 1602–1617 (1980).
22. Swift, J. & Hohenberg, P. C. Hydrodynamic fluctuations at the convective instability. *Phys. Rev. A* **15,** 319–328 (1977).
23. Hohenberg, P. C. & Swift, J. B. Metastability in fluctuation-driven first-order transitions: Nucleation of lamellar phases. *Phys. Rev. E* **52,** 1828–1845 (1995).
24. Murch, K. W., Moore, K. L., Gupta, S. & Stamper-Kurn, D. M. Observation of quantum-measurement backaction with an ultracold atomic gas. *Nature Phys.* **4,** 561–564 (2008).
25. Altman, E., Demler, E. & Lukin, M. D. Probing many-body correlations of ultra-cold atoms via noise correlations. *Phys. Rev. A.* **70,** 013603 (2004).
26. Horak, P. *et al.* Optical kaleidoscope using a single atom. *Phys. Rev. Lett.* **88,** 043601 (2002).
27. Salzburger, T., Domokos, P. & Ritsch, H. Enhanced atom capturing in a high-Q cavity by help of several transverse modes. *Opt. Express* **10,** 1204–1214 (2002).

Acknowledgements

This work was supported by NSF PHY08-47469 (B.L.L.), AFOSR FA9550-09-1-0079 (B.L.L.), DOE DE-FG02-07ER46453 (S.G.) and NSF DMR09-06780 (P.M.G.). P.M.G. gratefully acknowledges the hospitality of the Aspen Center for Physics.

Author contributions

All authors contributed equally to this work.

Additional information

Supplementary information accompanies this paper on www.nature.com/naturephysics. Reprints and permissions information is available online at http://npg.nature.com/reprintsandpermissions. Correspondence and requests for materials should be addressed to S.G.